JOURNAL OF CATALYSIS 114, 217–229 (1988)

The Location of Nickel Oxide and Nickel in Silica-Supported Catalysts: Two Forms of "NiO" and the Assignment of Temperature-Programmed Reduction Profiles

BRYNMOR MILE,* DIANE STIRLING,† MICHAEL A. ZAMMITT,† ANTONY LOVELL,‡ AND MAURICE WEBB‡

*Division of Chemistry, National Research Council of Canada, Ottawa, Ontario K1A 0R9, Canada; †Department of Chemistry and Biochemistry, Liverpool Polytechnic, Byrom Street, Liverpool L3 3AF, United Kingdom; and ‡Unilever Research Laboratory, Port Sunlight Laboratory, Quarry Road East, Bebington, Wirral, Merseyside LG3 3JU, United Kingdom

Received October 22, 1987; revised July 8, 1988

The preparation of nickel catalysts supported on a range of silicas results in the formation of two distinct types of "NiO" which reduce at very different temperatures under temperature-programmed reduction (TPR) conditions. Examination of the effects of pore structure and experiments designed to concentrate the oxides in either the smaller (~9 nm) or the larger pores (15–30 nm) show that the more reducible oxide is located mainly in the small pores and the less reducible oxide in the large pores. The more reducible oxide resembles bulk NiO and has negligible interaction with the silica. The less reducible oxide is either in the form of crystallites so small as to make nucleation of the reduction to metal difficult or as surface nickel silicates or hydroxysilicates. Reoxidation of the reduced catalyst followed by TPR shows that the nickel oxide and nickel crystallites are immobilized in the pores of the silica at temperatures up to 600°C.

INTRODUCTION

Despite its commercial importance there have been comparatively few systematic and basic studies of the preparation of supported catalysts. Basic research has been inhibited in part by the bewildering multiplicity of process variables at each stage and the apparent uniqueness of each system—hence the appellation "black art" to catalyst preparation. Fortunately there is now growing effort in this area as evidenced by the series of symposia on catalyst preparation (*1*) and a number of review articles (*2, 3*). We have undertaken a careful study of several stages of the preparation of silica-supported nickel catalysts. These were chosen because of their wide use (*4*) and because they have been extensively studied (*6*) since the classical work of Schuit and van Reijen (*5, 6*).

We have used a range of techniques to study the individual stages, but have found the relatively simple temperature-programmed reduction TPR) method (*7*) to be particularly useful as a diagnostic tool. However, there is always the problem of assigning the peaks of a TPR profile to definite chemical species or to the same species located in different sites in the support. In this paper we describe our attempts at such assignments (i) by using TPR in conjunction with other techniques, (ii) by studying silicas of widely different morphologies, and (iii) by employing a variety of simple pore modification techniques. In subsequent papers we will discuss how the TPR profiles change with changes in a number of preparation conditions and how they can be used to explain and to predict the activity and selectivity of the final catalyst.

EXPERIMENTAL

Catalyst preparation. Samples were prepared by impregnating the silicas with nickel nitrate solution followed by drying,

0021-9517/88 $3.00

calcining the nitrate to nickel oxide, and finally reducing it to nickel, usually in the TPR apparatus. The careful examination of the effects of variables at each stage will be discussed in Part II, so here we merely outline the procedures used in the present studies:

I. The silicas were pretreated at 120°C for 16 h immediately prior to impregnation to remove physically bound water.

II. The dried silicas were usually impregnated with five times the pore volume of the prescribed nickel nitrate solution either by dropwise addition or by spraying the vigorously stirred silica.

III. The impregnated silicas were normally dried in air at 120°C for 16 h and then calcined at 400°C for 3 h. X-ray diffraction (XRD) and thermal gravimetry (TG) showed that these conditions resulted in complete decomposition to nickel oxide (see below).

IV. The samples were cooled in air, stored under vacuum, and reduced in the TPR unit within 24 h of calcination. No differences were observed in samples reduced at varying times within this time period.

It is worth noting that when we attempted to use ion exchange methods with ammoniacal nickel nitrate solutions considerable dissolution and reprecipitation of the silicas and/or glassware occurred at the high pH needed. We decided to use the impregnation method in order to avoid the complications that might result, especially since we were particularly concerned in maintaining the integrity of the morphology and texture of the silicas.

Morphological characterization of silicas. Surface areas were determined with a Micromeritics Accusorb physical adsorption analyzer and application of the BET equation to nitrogen adsorption. A Quanta-Chrome scanning mercury porosimeter enabled the pore size distribution of the silicas to be estimated at each stage of preparation using standard techniques (*8*).

X-ray diffraction. A Philips 1700 automated X-ray diffractometer was used for both product identification and line broadening analysis to estimate particle sizes. Nickel-filtered copper $K\alpha$ radiation was selected and after data collection and file storage the "Sandman" software facility enabled the sample XRD to be compared to that of known compounds in the software library taken from the JCPDS index.

Thermogravimetry (TG), differential scanning calorimetry (DSC), and differential thermal analysis (DTA). The dehydration and decomposition of supported and unsupported nickel nitrate into nickel oxide were monitored using a DuPont TGA unit and a Perkin–Elmer DSC and DTA combined unit.

Determination of nickel content. The nickel was extracted by digestion with 20 cm^3 nitric acid (50%, w/w)/100 mg of sample on a steam bath for 4 h. After filtration and dilution the nickel content was determined by atomic absorption. The results were cross checked by gravimetric analysis using dimethylglyoxime and by X-ray fluorescence analysis of the undigested solid sample using a Philips P.W. 1400 spectrometer and a series of accurate standards prepared from dry mixes of nickel oxide and micronized Gasil-35 silica. Both test samples and standards were pressed into disks after addition of excess borax. The correspondence among the three methods was within 3%. Residual nickel not extracted from the silica by the nitric acid digestion was determined by dissolving the digested silica in hydrofluoric acid in a platinum crucible followed by dilution and atomic absorption to determine the Ni content.

Temperature-programmed reduction TPR (9, 10). A Perkin–Elmer sorptometer was adapted for TPR. The reactant stream (nitrogen (95%) and hydrogen (5%)) flowed downward over the sample supported on a the silica sinter in one arm of a vertical silica U-tube reactor surrounded by a tubular furnace whose temperature was increased linearly (12°C/min) using a Stanton Redcroft UTP Model programmer controlled

by a Chromel–Alumel thermocouple in contact with the sample. The loss of hydrogen from the reactant stream was detected by a katharometer whose voltage was fed into an integrator and a dual channel chart recorder whose other channel read the voltage from a separate Chromel–Alumel thermocouple in contact with the sample. Sample sizes were chosen so that they contained about 7 mg of reducible Ni. The proportionality between H_2 uptake and the amount of reducible oxide was checked by reducing a number of accurately known amounts of Ni(II) and Cu(II) oxides and found to be accurate to within 1% over the range used. The unit was calibrated dialy by injecting known amounts of H_2 into the N_2/H_2 carrier gas. With these precautions the TPR technique proved to be reproducible and quantitatively accurate in both peak position (±5°C) and hydrogen consumption (±2%).

Reoxidation of TPR reduced samples. In this series of experiments, after reduction in the TPR unit up to 620°C, the samples were reoxidized *in situ* by flowing gaseous oxygen at varying temperatures and for varying periods of time. A new TPR profile was then run on these oxidized samples.

RESULTS AND DISCUSSION

Micromeritics of Silicas Studied

The micromeritics of the silicas used (prepared by Unilever Research) are listed in Table 1. Impurity levels were as follows: 1000–2000 ppm of Al; <100 ppm of Mg, Ca, K; 10–100 ppm of Fe, Cu, Zn, Sr, Ba, P, S, U, F. Blank TPR experiments on the untreated silica showed no reduction peaks. It is convenient to discuss the silicas used in this work in terms of primary (1.5-nm), secondary (15-nm), and tertiary (150-nm) silica particles and their associated pores. Each larger particle is built from the smaller particles, the tertiary particles themselves being loosely bound within quaternary particles of 100 μm in size in unmicronized and 5 μm in micronized silicas (i.e., after milling) (*11*) (Fig. 1). The range of silicas was selected to study the effect of a wide range of pore diameters on TPR profiles and other properties.

TABLE 1

Micromeritics of Silicas Used

Silica	Mean pore diameter (nm)	Pore volume ($cm^3\ g^{-1}$)	Surface area ($m^2\ g^{-1}$)
Sorbsil	<2	0.4	800
HP34	15	1.64	260
Gasil-35 micronized	16	1.55	300
UHPV	25	2.15	340
SD116	28	2.11	323

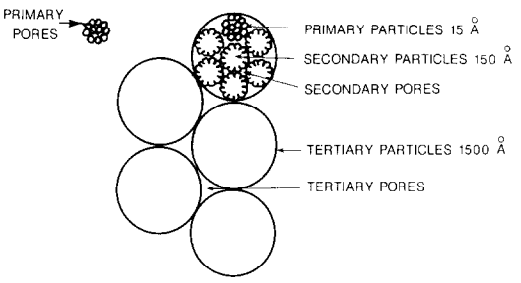

FIG. 1. Schematic representation of the particle and pore structure of the silicas used.

Porosimetry examination of the pore structures of the silicas after each stage of catalyst preparation showed that there was little change (<5%) for the more robust silicas (e.g., Gasil-35). For the very high-porosity silicas (e.g., UHPV) the degree of structural rearrangement depended on the severity of the drying conditions; slow oven drying produced a 16% drop in pore volume and a 35% reduction in the mean pore diameter, largely because of some collapse of the tertiary pore structure.

Thermal and XRD Studies of the Calcination of Nickel Nitrate

The thermal decomposition of nickel nitrate to nickel oxide is a complex multistep solid-phase reaction (*12–14*) and many of these steps could be affected by the support by changes in nucleation site density, nu-

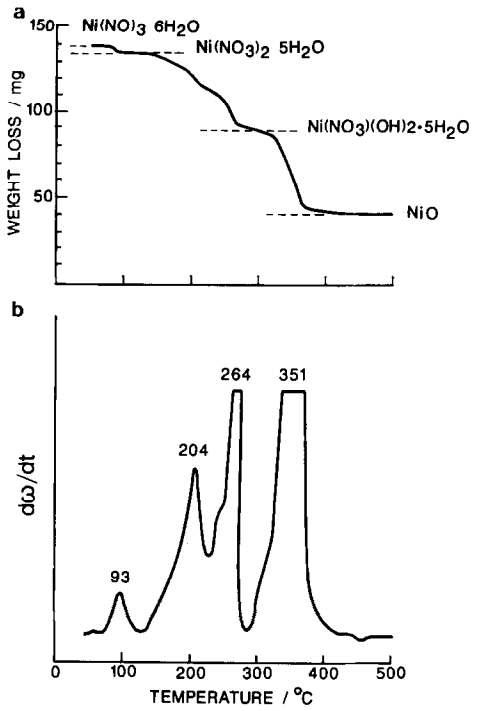

FIG. 2. (a) TGA of the thermal decomposition of unsupported $Ni(NO_3)_26H_2O$. Ramp rate 10°C min^{-1}; (b) first derivative of TGA curve 2 (a).

cleation rate, and the rate of NiO crystal growth. TGA, DSC, and XRD techniques were used to study the calcination of silica-supported and unsupported nickel nitrate.

Figure 2 shows the TGA traces for bulk nickel nitrate. The following three main decomposition stages can be distinguished (percentage weight loss theoretical *T* and experimental *E* shown in parentheses):

I. $Ni(NO_3)_26H_2O \rightarrow (-H_2O/(93–125°C))$ $Ni(NO_3)_25H_2O$ (*T*, 3.0%; *E*, 2.6%).

II. $Ni(NO_3)_25H_2O$ $((-HNO_3, -1.5\ H_2O)/(125–265°C)) \rightarrow Ni(NO_3)(OH)2.5H_2O$ (*T*, 31.0%; *E*, 30.3%).

III. $Ni(NO_3)(OH)2.5H_2O$ $((-HNO_3, -2.5\ H_2O)/(285–425°C)) \rightarrow NiO$ (*T*, 37.1%; *E*, 36.5%).

Stage II consists of at least three steps, the first two involving mainly the loss of water and the last the loss of nitrate to give the basic nickel nitrate intermediate $Ni(NO_3)(OH)2.5H_2O$. Keeley and Maynor (*12*) also reported such an intermediate but with one less water molecule, $Ni(NO_3)(OH)1.5H_2O$. The DTA of nickel nitrate confirmed the occurrence of endothermic changes at 254 and 351°C but the loss of the first water of hydration at 93°C could not be distinguished.

Figure 3 shows the corresponding TGA for $Ni(NO_3)_26H_2O$ supported on micronized Gasil-35 at a 13% nickel loading. Three primary stages are again clearly distinguished with a multiplicity in stage II, the basic nitrate being again clearly indicated. The most significant difference is the much lower temperature for the occurrence of each change for the supported nitrate, the maximum rate for each case being observed at the following temperatures: 93 and 83°C, 204 and 162°C, and 351 and 264–286°C. DTA confirmed the lowering of the temperature for each decomposition stage. The rate enhancement by the support could be due to an increase in lattice defects and nucleation site densities in the small blocks of Ni(II) on the surface. However, it is also possible that the enhancement has a more chemical basis and arises from reaction of

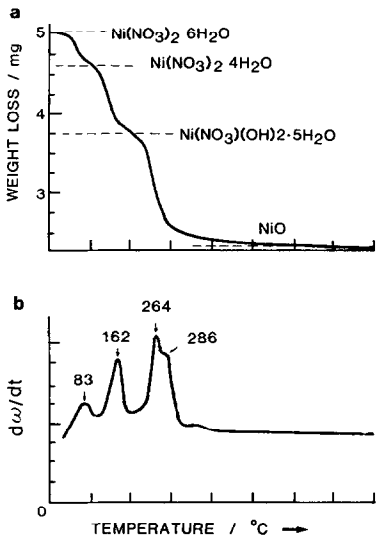

FIG. 3. (a) TGA of $Ni(NO_3)_26H_2O$ supported on Gasil-35 (8.3% (w/w) loading); (b) first derivative of TGA curve 3(a).

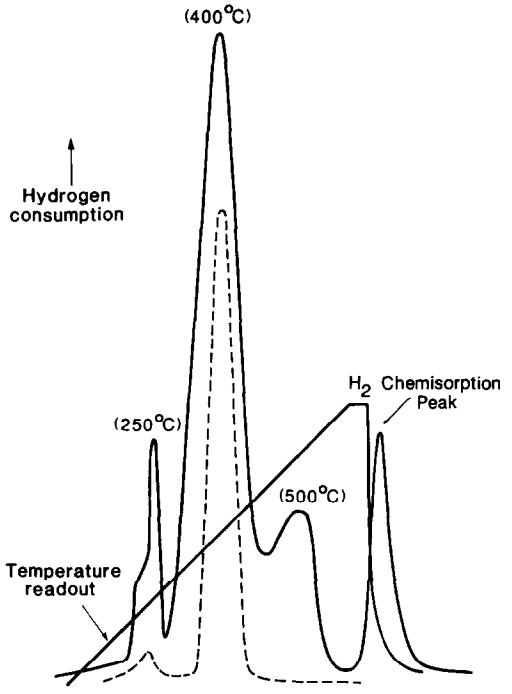

FIG. 4. (a) (---) TPR of unsupported NiO; (b) (—) TPR of "NiO" supported on micronized Gasil-35 (8.8% (w/w) loading). TPR conditions: 60 mg of sample; ramp rate 12°C min^{-1}, 5% H_2N_2 calcination at 400°C for 16 h.

the silica surface, probably via surface OH groups, with nickel nitrate or basic nitrate to form surface nickel silicates or hydroxy silicates.

XRD examination of supported samples quenched at each of the three stages showed the formation of $Ni(NO_3)_2 4H_2O$ and the final production of cubic bunsenite NiO particles of ~10 nm in size. There was no definitive evidence for the basic nitrate intermediate detected by TGA or for nickel silicates or nickel hydroxysilicates, although weak broad reflections were possibly present at the correct reflections.

Temperature-Programmed Reduction

As shown in Fig. 4 the TPR of bulk nickel oxide consisted of a single reduction peak at 400°C slightly skewed toward lower temperatures. The peak at 250°C was small (<1%) and erratic and sometimes was not present. The example of the TPR of supported nickel oxide (8.8% (w/w) of Ni on micronized Gasil-35) in Fig. 4 shows the marked effect of the support in producing a number of peaks and broadening the whole profile to much higher temperatures. There are three reduction peaks at 250, 400, and 500°C and a chemisorption peak at ~260°C obtained on cooling the sample from 600°C to ambient in the N_2/H_2 carrier gas stream.

Peak I (250°C) can be assigned unambiguously to the reduction of traces of the higher Ni(III) oxide; the intensity of this peak corresponded to increased amounts of black "Ni_2O_3" clearly visible against the pale green NiO and was absent in the TPR of samples showing no traces of the higher oxide. Its occurrence or nonoccurrence did not affect the remainder of the TPR profile. Peak II (400°C), which we will refer to as the low-temperature peak (LT), occurs at the same temperature as the unsupported nickel oxide and therefore is probably due to large crystallites of bulk nickel oxide interacting hardly at all with the silica support which merely acts as a dispersing agent. Peak III (500°C), which we will refer to as the high-temperature peak (HT), reduces 90–100°C higher than bulk NiO and clearly results from a much more difficultly reduced Ni(II) species. The summed H_2 consumption of the LT and HT peaks corresponds to complete reduction of the measured amount of nickel in the sample to Ni(0). The Ni(II) species responsible for the HT peak could be either a surface nickel silicate or NiO present as very small, difficulty reducible particles. We discuss these alternatives in detail below. Similar, although less well-resolved, TPR profiles have been reported by others (*7, 15*) but not discussed. The relative proportions and sometimes the positions of the LT and HT peaks are highly sensitive to some preparation conditions and insensitive to others and also correlate with the activity and selectivity of the final nickel catalyst (to be presented in Part II). Before considering the chemical nature of the two Ni(II) spe-

cies and their location in the silica pore structure we discuss briefly a perquisite of the TPR technique, the hydrogen chemisorption peak observed on cooling the reduced sample in the N_2/H_2 stream.

The Hydrogen Chemisorption Peak

Following McNicol and co-workers (*16*), we assign the peak observed at ~260°C on cooling to H_2 uptake by chemisorption on the surface of the nascent nickel particles just formed during the TPR reduction but denuded of surface hydrogen at the maximum temperature of 620°C. There is no other apparent explanation and it seems reasonable in the light of the known desorption and adsorption characteristics of H_2 on supported nickel catalysts (*17*). If this interpretation is correct the peak can be used to determine the nickel surface area and to give an estimate of particle size directly from a single TPR experiment. In order to justify the use of the chemisorption peak for this purpose we determined the nickel surface area of representative samples by traditional H_2 chemisorption measurements and found the monolayer volume of H_2 to be within ±10% of that determined from the TPR chemisorption peak. Coenen and Linsen's equation, $S_{Ni} = 3.4V_m$ ($m^2\ g^{-1}$ (*6*) was used to determine the specific nickel surface area, S_{Ni}, from the volume of chemisorbed H_2, V_m (corrected to STP). Assuming the nickel particles to be hemispherical, their mean diameter, $\bar{d}$ (nm), is related to S_{Ni} by $\bar{d} = 431/S_{Ni}$ (*6*). A further check was to estimate the Ni particle size by X-ray line broadening. Reasonable agreement was found for the samples containing large particles with XRD giving $\bar{d}$ = 16 nm and H_2 chemisorption 12 nm but, as expected, discrepancies appeared for particles below ~5 nm with XRD and H_2 chemisorption giving 9 and 2 nm, respectively. Parkash (18) has shown that XRD gives larger size estimates than chemisorption because the two techniques give volume and surface averages, respectively. It is possible that the large difference between the chemisorption and XRD-determined sizes may indicate a bimodal distribution. Mustard and Bartholomew (*19*), from their thorough investigation of sizing techniques, conclude that H_2 chemisorption provides the most accurate method because of its sensitivity to the smaller particles. The nickel particle diameters reported in this paper are based on the H_2 chemisorption peak.

TABLE 2

TPR Characteristics of Nickel on Various Silicas

Silica	Sorbsil	HP34	Gasil-35	UHPV
1% (w/w) nickel on silica (micronized)				
Mean pore diameter (nm)	<2	15	16	25
% LT peak	68	61	42	29
% HT peak	32	39	58	72
$\bar{d}$(nm)	1.5	1.3	0.8	0.9
9% nickel on silica (micronized)				
% LT peak	—	92	88	—
% HT peak	—	8	12	—
$\bar{d}$(nm)	—	7.2	6.0	—

Silica Micromeritics and the TPR of Supported NiO

The effects of the mean pore diameter of the silicas on the proportions of the LT and HT TPR peaks and final nickel particle size are summarized in Table 2. Surprisingly, the LT peaks decreased and the HT peaks increased with an increase in pore diameter, suggesting that the LT peak is associated with the small pores and the HT peak with the large pores of the silica. The Sorbsil contains virtually no secondary or tertiary particles and hence is too extreme a case to correlate with the other silicas. A more detailed study of pore structure is shown in Table 3 for three forms of silica, Gasil-35, UHPV, and SD116. The number of moles of Ni per gram in the secondary and tertiary pores (columns 6 and 7) is that calculated from the total nickel content proportioned according to the respective pore volumes of these pores. The almost exact correspondence of these numbers with the

TABLE 3

Pore Structure and TPR of Nickel Catalysts (1%) Supported on Micronized Gasil-35, UHPV, and SD116 Silicas

Silica	Secondary pores		Tertiary pores		Ni content[a]		Ni content	
	Pore volume ($cm^3\ g^{-1}$)	Mean diameter (nm)	Pore volume ($cm^3\ g^{-1}$)	Mean diameter (nm)	Sec. pores ($mg\ g^{-1}$)	Tert. pores	LT peak ($mg\ g^{-1}$)	HT peak
Gasil-35	0.65	8.8	0.90	35.5	4.2	5.8	4.2	5.8
UHPV	0.60	7.0	1.55	47.3	2.8	7.2	2.9	7.1
SD116[b]	0.59	8.7	1.52	54.4	2.8	7.2	4.3	5.7

[a] Calculated from total nickel loading and proportioned according to pore volumes.
[b] SD116 freeze dried to maintain pore integrity.

number of moles of Ni(II) associated with the LT and HT peaks in Gasil-35 and UHPV is perhaps fortuitous but strongly suggests that the Ni(II) of the LT peak is located in the small, secondary pores while that of the HT peak is in the larger, tertiary and quaternary pores. Although in the right direction, the results for SD116 silica show a poorer correspondence; this may be associated with the different drying technique used. The results suggest that, at the 1% level, nickel ions do not transfer from one pore to another by capillary action during drying. This indicates chemical binding to the silica surface presumably through the involvement of surface hydroxyls. In order to provide further evidence for the rather unexpected conclusion regarding the location of the two Ni(II) species we conducted three sets of experiments aimed at specifically skewing the Ni(II) distribution into either the large or the small pores.

Autoclaving

Here the purpose was to change the distribution of pore sizes before impregnation. SD116 silica was subjected to hydrothermal treatment in an autoclave at 260 psi for 1 h at 210°C in order to reduce the smaller primary and secondary pores and favor the larger tertiary pores (*11*). Mercury porosimetry showed an increase in the mean secondary pore diameter from 8.7 to 22.3 nm and in the tertiary pore diameter from 54.4 to 136.0 nm. TPR showed an increase in the HT peak from 65 to 90%, in agreement with this peak being associated with the metal oxide in the larger pores.

The Effects of Using Impregnation Volumes below the Pore Volume

Silica SD116 samples were treated with the pore volume and with 50 and 20% of the pore volume of $NiNO_3$ solutions to give a final nickel loading of 1% in each case. A spray technique with vigorous agitation of the silica was used to ensure homogeneity, other conditions being held constant. We anticipated that the nickel nitrate solution would tend to collect in the smaller pores by capillary action and hence the peak associated with oxide in the smaller pores would be enhanced in the 50 and 20% cases. The results showed that the LT peak did indeed increase as less than the pore volume was used.

Volume used	Pore volume	50% Pore volume	20% Pore volume
% LT Peak	35	65	67
% HT Peak	65	35	33

Pore Blocking Experiments

Here we attempted to fill the tertiary pores with the nickel salt by blocking the smaller pores either with an organic solvent immiscible with water or with ice. In the first method we followed the technique de-

vised by Gregg and Tayyab (*20*) for micropore determination. Nonane (0.5 $cm^3\ g^{-1}$) was added to the silica to fill the small pores (this being the volume of the smaller pores determined by porosimetry); the remaining, tertiary, pores were then filled with aqueous nickel nitrate solution (1.3 $cm^3\ g^{-1}$). In the second method the small pores were filled with water (0.5 $cm^3\ g^{-1}$) which was then frozen into the pores using a dry-ice slush bath. A sufficient amount of methanol solution of nickel acetylacetonate was then added to fill the tertiary pores. Both samples were freeze dried before calcining. Separate experiments using a nickel acetylacetonate methanol solution were run as a control. Neither method will lead to a clear demarcation between the small and the large pores but trends should be observable. The results revealed an increasing preponderance of the HT peak when the nickel salt was "foreced" preferentially into the larger pores using either method.

	Control	Nonane blocking	Ice blocking
% LT peak	43	<5	11
% HT peak	57	>95	89

Taken alone none of these results provide definitive proof but together they do constitute good evidence for the unexpected conclusion that the more readily reduced Ni(II) is located mainly in the small pores and the less readily reduced Ni(II) is in the large pores. Before discussing the reasons for this preferred location the nature of the two reducible forms of Ni(II) needs to be considered.

The Nature of the Supported Nickel "Oxide"

The low-temperature peak. The correspondence between the peak maximum of the LT peak and that of the bulk nickel oxide makes it reasonable to assign this peak to large particles of nickel oxide which, although well dispersed by the silica, do not form significant chemical bonds with the underlying surface. Delmon and others (*21–23*) have proposed a similar assignment of the spontaneously reducible NiO found in their isothermal reduction studies of silica-supported nickel species.

The High-temperature peak. In addition to an irreducible nickel silicate (~5% of the total nickel content) Delmon *et al.* also found evidence for a NiO which was far less reducible than the bulk oxide and which they called initiable nickel oxide (*21–23*). They proposed that this was an oxide present as very small particles and that the difficulty of reduction arose from the low rate of nucleation of these small-sized particles. The arguments in favor of this proposal were plausible but qualitative with no direct evidence being available. A similar two-particle model has been proposed by Burch and Collins for the decreased reactivity of molybdenum oxide supported on alumina (*24*). Such an explanation is also possible for the HT peak observed in the present work. However, we favor a more chemical reason for the HT peak, namely the formation of amorphous surface nickel silicates or nickel hydroxysilicates bearing some resemblance to bulk silicates. Thomas *et al.* (*25*) have suggested similar surface compounds to explain the decreased reducibility of Mo/Al_2O_3 catalysts. Likewise Dalmon *et al.* proposed a similar explanation for the inhibition of nickel reduction on silica and alumina (*23*). The interaction is probably similar to that designated medium (MMSI) by Bond (*26*) as opposed to strong (SMSI) and weak metal support interaction (WMSI). The differences at the low particle size ~1 nm may actually be semantic since for hemispherical particles ~30% of the nickel oxide phase will be in contact with the silica surface and even greater proportions will be in contact for raft-like particles. Such intimate contact between the two phases must result in moderately strong interaction even if only by charge transfer processes and could lead to a reducibility intermediate between bulk nickel oxide and nickel silicates; i.e.,

the extensive interface acts as a "chemical" glue as proposed by Coenen and Linsen (*6*) and helps to reduce sintering and maintain a high metal dispersion. The recent careful magnetic studies of silica-supported nickel particles have shown that small amounts of Ni^+ and Ni^{2+} at the nickel/silica interface have an anchoring effect and reduce sintering (*27*). We discuss the two models briefly.

The two-particle size model. Perhaps the strongest evidence in favor of this model is negative in that no well-defined XRD reflections from a nickel silicate or basic silicate were observed by Delmon *et al.* (*21, 22*) or by us. We have also found that all the nickel is extractable with dilute HNO_3 from samples calcined at <400°C whereas nickel silicates are not extractable. Additionally we found that prepared nickel silicates do not begin to reduce until 550°C whereas the HT species peaks at 500°C and is completely reduced by 550°C. Hence bulk silicates are certainly not formed or responsible for the HT peak. However, the absence of well-defined nickel silicate XRD reflections does not preclude the presence of thin layers of amorphous surface nickel silicates at the 1% level. Direct support for the two-particle size model comes from the careful X-ray diffraction studies of Ganesan *et al.* (*28*) who found a biomodal distribution of nickel oxide particles in NiO/SiO_2 systems.

The Surface Silicate Model

There are many examples of oxide/support interactions: Pt-aluminate in Pt/Al_2O_3 (*29*), Fe_3O_4 on silica (*30*), and Mo(VI) on silica and alumina (*31*). Nickel silicates are formed in catalysts prepared by precipitation (*6*) and probably by ion exchange (*32*) but to our knowledge there is no evidence for silicate formation in silica catalysts prepared by impregnation. Nickel aluminates are formed on alumina supports (*33, 34*) and we have found that nickel catalysts prepared by impregnation on alumina are only reduced above 700°C under TPR conditions. Recent theoretical calculations suggest that moderate chemical bonding can also occur between nickel and a silica surface (*35*).

The large temperature differences (~100°C) found in this work between the LT and HT peaks are indicative of a chemical difference between the species responsible. Two other observations also support this conclusion.

(i) Increasing the time and/or temperature of the calcination stage causes an increase in the proportion of the HT peak and a diminution in the nickel particle size. This aspect will be discussed in detail in Part II but, for example, increasing the calcination temperature of a 1% Ni on Gasil-35 catalyst from 400 to 600°C resulted in the HT peak proportion increasing from 40 to 60% and to the particle size decreasing from 10 to 2.5 nm. Both effects can be readily understood by an increased extent of reaction of the NiO with the silica to form surface silicates which are less mobile and hence lead to higher dispersions of the nickel metal. The two-particle size model predicts that an increase in calcination temperature should promote the formation of larger, thicker nickel oxide particles (i.e., more of the LT peak) and hence larger nickel crystallites in contradiction to experiment.

(ii) Increasing the nickel loading on Gasil-35 from 1 to 31% resulted in an increase in the amount of nickel oxide in the HT peak from 306 to 860 μmol g^{-1}, but the major proportion of the additional nickel was associated with the LT peak which increased from 22 to 9360 μmol g^{-1}. If the two-particle size model were applicable, the amount of nickel in the HT peak would be expected to diminish with a 30-fold increase in the surface concentration of the oxide since large numbers of small particles should aggregate to larger particles under these conditions. The surface nickel silicate model provides an explanation if only a small proportion of the surface in the large pores can form the surface silicates. Interestingly, if we assume five OH groups/100 $Å^2$ (*11, 36*) we

TABLE 4

Calculated Percentage Monolayer Coverage in Small and Large Pores

Nickel loading (%)	Gasil-35		UHPV		SD116	
	Sec. pores	Tert. pores	Sec. pores	Tert. pores	Sec. pores	Tert. pores
1	1.1	3.7	0.7	4.0	0.8	4.8
10	11	37	7	40	8	48

calculate there to be 840 μmol g^{-1} of OH groups in the large tertiary pores of Gasil-35. The closeness of this to the limiting value of 860 μmol g^{-1} of Ni in the HT peak is probably fortuitous but it would appear that the silicates could be formed at surface hydroxyl sites and it is possible that the basic nickel nitrate intermediate is involved in this surface reaction although a simple ion exchange reaction could also occur. However, it is difficult to see why the larger amounts of surface OH groups in the smaller secondary pores (~2500 μmol g^{-1}) do not react similarly. We now address this problem

Differences between "NiO" in Small and Large Pores

A simple explanation would be that the crystallites of "NiO" readily coalesce to bulk-like NiO in the small pores which are of comparable size (~10 nm) whereas in the larger pores (>100 nm) they are dispersed on the larger perimeter and remain discrete. We have calculated the monolayer coverages in the secondary and tertiary pores on the basis of the following simplifying assumptions: the pores are open-ended cylindrical capillaries; there is no capillary flow during drying, the Ni^{2+} ions being immobilized in their initial pores; all the surface is amenable to "NiO" deposition; the NiO monolayer has a thickness of 0.27 nm. The calculated percentage monolayer coverage for three silicas at 1 and 10% Ni loading are shown in Table 4. There is insufficient NiO even at 10% loading to give monolayer coverage. The percentage monolayer coverage is calculated to be greater in the larger than in the smaller pores and hence there should be more of a tendency for aggregation to bulk NiO in the larger pores which is in the opposite direction to that needed to explain the TPR results. If appreciable capillary flow occurs during drying the nickel ions will accumulate more in the smaller pores and this could lead to larger, more bulk-like, NiO in these pores. The results already presented in Table 3 for 1% loading indicate that such mobility probably does not occur. The 1% loading is similar to the loadings produced by cation exchange methods using alkaline ammoniacal solutions and which also result in nickel particle sizes (<2–3 nm) similar to those found here at 1% loading. It thus seems possible that at the low loading similar chemical interaction with the silica surface is occurring either by cation exchange or by reaction of a basic nickel nitrate as already suggested. However, such interactions should also occur in the small pores whereas experimentally it appears that noninteracting, bulk NiO predominates. Three speculations are offered. First, the assumption that all the silica surface is amenable to "NiO" coverage is probably invalid and the number of such sites suitable for NiO growth may be different in the small and large pores. Second, separate crystals grow from such low density sites and, whereas in the small pores these connect with each other to form a network of crystallites with properties similar to those of bulk NiO, in the large pores with longer perimeters such enmeshing of crystallites does not occur. However, at higher loadings networks form even in the large pores. Third, steric effects could inhibit silicate or hydrosilicate formation in the smaller pores because of the lamellar structure of these intermediates.[1]

[1] We are grateful to a referee for suggesting this possibility.

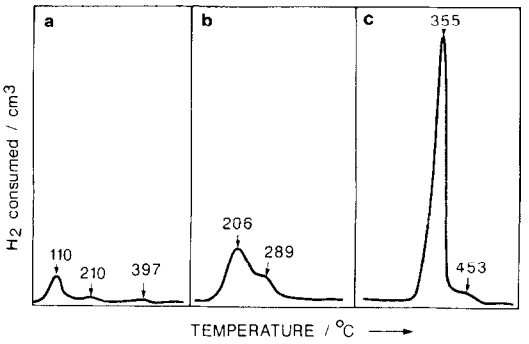

FIG. 5. TPR of samples after reoxidation of previously reduced catalyst. (8.3% (w/w) Ni on micronized Gasil-35). (a) TPR of reduced sample after O_2 treatment at 28°C. (b) TPR of reduced sample after O_2 treatment at 260°C for 30 min. (c) TPR of reduced sample after O_2 treatment at 400°C for 16 h.

TPR of Reoxidized Samples

Samples were taken through the following sequence: TPR up to 620°C, cool down in N_2/H_2, oxidation in an O_2 stream for varying times and temperatures, repeat of the TPR up to 600°C without removing the samples from the TPR unit. The object was to determine whether such oxidation changed the nature and the location of the nickel. They also served to check the use of the H_2 chemisorption peak as a measure of particle size. The results are illustrated in Fig. 5 and summarized in Table 5.

The TPR of samples reoxidized at 25°C was independent of oxidation time and consisted of two low-temperature peaks at 110 and 210°C followed by a small broad tail extending to about 440°C. Hydrogen consumption was 12% of the parent sample and 3.8 times larger than the hydrogen chemisorbed on cooling. It seems very likely that the TPR is that of a surface nickel oxide with 88% of the nickel remaining unoxidized in the interior of the metal particle. Assuming that the TPR peaks correspond to a process with stoichiometry NiO (surface) + $1.5H_2 \rightarrow$ NiH(s) + H_2O the hydrogen consumption should be three times that of the chemisorption peak, Ni(s) + $\frac{1}{2}H_2 \rightarrow$ NiH(s). The larger experimental value of 3.8 could be due to reaction with chemisorbed molecular oxygen or arise because some oxidation of subsurface nickel has occurred. Estimates of oxidation penetration of the surface range from 1 (*6*) to 1.8 monolayers (*37*). The 25°C oxidation results appear to confirm the validity of using the H_2 chemisorption peak for surface area measurements. A similar titration technique has been used by Burwell and co-workers (*38*). An interesting feature of the 25°C reoxidation results is the observation of not one but two TPR peaks resembling the two peaks of the parent sample but displaced to much lower temperature. It seems that the reducibility of even the surface nickel oxide is controlled by the environment of the parent oxide.

The TPR of samples reoxidized at higher temperatures depended on the duration of the oxidation. After 30 min of oxidation at 260°C the TPR profile was similar to that of the 25°C oxidation but with the peaks moved to higher temperatures (206 and 289°C) and with a H_2 consumption of 53% of that in the parent TPR peaks. Clearly oxidation beyond the surface layer had occurred and the lowering of the peak temperatures below those of the original TPR probably results from activation of the hydrogen by the 47% unoxidized nickel; the black color of the sample even after reoxidation was indicative of the presence of appreciable amounts of metallic nickel.

TABLE 5

TPR of Samples of 8.8% (w/w) Ni on Gasil-35 Reoxidized with Gaseous O_2

Oxidation conditions	Parent sample	25°C 8 days	260°C 30 min	260°C 16 h	400°C 16 h
% LT	86	74	68	48	90
Peak	(395)[a]	(110)	(200)	(290)	(360)
% HT	14	26	32	52	10
Peak	(495)	(210)	(350)	(380)	(450)
Particle diameter (nm)	10.7	—	—	8.4	9.8

[a] Temperature in °C of peak maximum in parentheses.

Reoxidation at 400°C for 16 h gave a sample having the characteristic pale green color of nickel oxide, which had a TPR profile similar to that of the parent TPR but with the LT and HT peaks occurring about 40°C lower but having similar proportions. H_2 consumption was within 6% of the parent TPR peak and the final nickel particle size of 10 nm was virtually identical to that of the parent particle size of 11 nm. A small difference between the parent TPR and the fully oxidized sample is to be expected because of the very different routes to the oxides which could produce differences in lattice defects and support interactions. Indeed, the similarity is the more interesting feature since it shows that neither the nickel oxide nor the nickel particles are mobile on Gasil-35 silica during reduction at 620°C or during oxidation at 400°C. This indicates a medium to fairly strong metal/support interaction (MMSI, SMSI). This contrasts with the results for the reoxidation of nickel and copper particle in X and Y zeolites where extensive migration to the surface occurred (*39, 40*).

CONCLUSIONS

1. Nickel nitrate incorporated into porous silicas by impregnation decomposes by a multistep process to form "nickel oxide" via a basic hydroxynitrate Ni $(NO_3)(OH)2.5H_2O$; the silica support reduces the temperatures required for each calcination stage.

2. Two distinct types of "NiO" are formed and are distinguished by a temperature difference of ~100°C in their peak maxima during TPR.

3. The more reducible "NiO" resembles bulk nickel oxide and is probably in the form of large crystallites which are dispersed by, but do not interact chemically with, the silica surface.

4. The less reducible "NiO" either is in the form of small crystallites that inhibit nucleation or is a surface nickel silicate or hydroxysilicate.

5. The more reducible "NiO" is located mainly in the small pores with mean diameters of ~9 nm and the less reducible oxide is located in the large pores with mean diameters of 20–30 nm.

6. Reoxidation of the final nickel particles formed by reduction of both oxides results in a return to the original oxides in their original locations in the two types of pores showing that the nickel does not migrate to the surface but is immobilized within the pore framework at 620°C.

REFERENCES

1. "Scientific Bases for the Preparation of Heterogeneous Catalysts," 4th International Symposium, Louvian-la-Neuve, Belgium, Sept. 1986, and previous quadrennial symposia.
2. Komiyama, M., *Catal. Rev. Sci. Eng.* **27,** 341 (1985).
3. Lee, S. Y., and Rutherford, A., *Catal. Rev. Sci. Eng.* **27,** 207 (1985).
4. Dewing, J., and Davies, D. S., "Advances in Catalysis" (D. D. Eley, P. W. Selwood, and P. B. Weisz, Eds.), Vol. 24, p. 234. Academic Press, New York, 1975.
5. Schuit, G. C. A., and van Reijen, L. L., "Advances in Catalysis" (W. G. Frankenburg, V. I. Komarewsky, and E. K. Rideal, Eds.), Vol. 10, p. 242. Academic Press, New York, 1958.
6. Coenen, J. W. E., and Linsen, B. G., "Physical and Chemical Aspects of Adsorbents and Catalysts," p. 472, Academic Press, London/New York, 1970.
7. Robertson, S. D., McNicol, B. D., de Baas, J. H., Kloet, S. C., and Jenkins, J. W., *J. Catal.* **37,** 424 (1975).
8. "Characterisation of Powder Surfaces" (G. D. Parfitt and K. S. W. Sing, Eds.) Academic Press, London/New York, 1976.
9. Hurst, H. N., Gentry, S. D., Jones, A., and McNicol, B. D., *Catal. Rev. Sci. Eng.* **24,** 233 (1982); Jones, A., and McNicol, B. D., "Temperature Programmed Reduction for Solid Materials Characterization," Chemical Industries Series, Vol. 24. Dekker, New York, 1986.
10. Monti, D. A. M., and Baiker, A., *J. Catal.***83,** 323 (1983).
11. Barby, D., "Characterization of Powder Surfaces" (G. D. Parfitt and K. S. W. Sing, Eds.) p. 353. Academic Press, London/New York, 1976.
12. Keely, W. M., and Maynor, H. W., *J. Chem. Eng. Data* **8**(3) 297 (1963).
13. Weigel, D., Imelik, B., and Laffitte, P., *Bull. Soc. Chim. Fr.*, 345 (1962).
14. Burch, R., and Flambard, A. R., *in* "Preparation of Catalysts III," Proc. 3rd Intern. Symp. on

Preparation of Catalysts, Louvain-la-Neuve, 1982 (G. Poncelet, P. Grange, and P. A. Jacobs, Eds.), p. 311. Elsevier, Amsterdam, 1983.
15. Unmuth, E. E., Schwartz, L. H., and Butt, J. B., *J. Catal.***61,** 242 (1980).
16. McNicol, B. D., private communication.
17. Konvalinka, J. A., Oeffelt, P. H., Scholten, J. J. F., *Appl. Catal.* **1,** 141 (1981).
18. Parkash, S., *Chem. Tech.* **10**(9), 572 (1980).
19. Mustard, D. G., and Bartholomew, C. H., *J. Catal.* **67,** 186 (1981).
20. Gregg, S. J., and Tayyab, M. M., *J. Chem. Soc. Faraday Trans. 1* **74,** 348 (1978).
21. Delmon, B., and Roman, A., *J. Catal.* **30,** 333 (1973).
22. Houalla, M., and Delannay, F., Matsuura, I., and Delmon, B., *J. Chem. Soc. Faraday Trans. 1* **76,** 2128 (1980).
23. Turlier, P., Praliaud, H., Moral, P., Martin, G. A., and Dalmon, J. A., *Appl. Catal.* **19,** 287 (1985).
24. Burch, R., and Collins, A., *Appl. Catal.* **18,** 389 (1985).
25. Thomas, R., de Beer, V. H. J., Medema, J., and Moulijn, J. A., *J. Catal.* **76,** 241 (1982).
26. Bond, G. C., "Metal Support and Metal Additive Effects in Catalysts" (B. Imelik, C. Naccache, G. Coudurier, H. Praliaud, P. Meriaudeau, P. Gallezot, G. A. Martin, and J. C. Vedrine, Eds.). Elsevier, Amsterdam, 1982.
27. Bonneviot, L., Olivier, M. C. D., Martin, G. A., and Freund, E., *J. Phys. Chem.* **90,** 2112 (1986).
28. Ganesan, P., Kuo, H. K., Saavedra, A., and de Angelis, R. J., *J. Catal.* **52,** 310 (1978).
29. Yao, H. C., Sieg, M., and Plummer, H. K., *J. Catal.* **59,** 365 (1979).
30. Lund, C. R. F., and Dumesic, J. A., *J. Catal.* **72,** 21 (1981).
31. Rodrigo, L., Marcinkowska, A., Adnat, A., Roberge, P. C., Kaliaguine, S., Makovsky, L. E., Diehl, J. R., and Stencel, J. M., *J. Phys. Chem.* **90,** 2690 (1986).
32. Turlier, P., Dalmon, J. A., and Martin, G. A. "Metal Support and Metal Additive Effects in Catalysis" (B. Imelik, *et al.*, Eds.), p. 203. Elsevier, Amsterdam, 1982.
33. Ross, J. R. H., Steel, M. C. F., and Zeini-Isfahani, A., *J. Catal.* **52,** 280 (1978).
34. Bartholomew, C. H., Pannell, R. B., and Butler, J. L., *J. Catal.* **65,** 335 (1980).
35. Haberlandt, H., and Ritschl, F., *J. Phys. Chem.* **90,** 4322 (1986).
36. Snoeyink, V. L., and Weber, W. J., *Prog. Sur. Membr. Sci.* **5,** 63 (1972); Boehm, H. P., "Advances in Catalysis" (D. D. Eley, P. W. Selwood, and P. B. Weisz, Eds.), Vol. 16, p. 179. Academic Press, New York, 1966.
37. Richardson, J. T., and Dubus, R. J., Crump, J. G., Desai, P., Osterwalder, H., and Cale, T. S., *in* "Preparation of Catalysts II," Proc. 2nd Intern. Symp. on Preparation of Catalysts, Louvain-la-Neuve, 1978 (B. Delmon, P. Grange, P. Jacobs, and G. Poncelet, Eds.), p. 131. Elsevier, Amsterdam, 1979.
38. Kabayashi, M., Inoue, Y., Takahashi, N., Burwell, R. L., Butt, J. B., and Cohen, J. B., *J. Catal.* **64,** 74 (1980).
39. Jacobs, P. A., Linart, J. P., Nijs, H., and Uytterhoeven, J. B., *J. Chem. Soc. Faraday Trans. 1* **73,** 1745 (1977).
40. Gentry, S. J., Hurst, N. W., and Jones, A., *J. Chem. Soc. Faraday Trans. 1* **75,** 1688 (1979).